Catalysis Letters Vol. 105, Nos. 3–4, December 2005 (© 2005)
DOI: 10.1007/s10562-005-8681-x

Fabrication of dense arrays of platinum nanowires on silica, alumina, zirconia and ceria surfaces as 2-D model catalysts

X.-M. Yan[a,*], S. Kwon[b], A.M. Contreras[a,c], M.M. Koebel[c], J. Bokor[b,e] and G.A. Somorjai[a,c,d]

[a]*Department of Chemistry, University of California, Berkeley, 94720 CA*
[b]*The Molecular Foundry, Lawrence Berkeley National Laboratory, Berkeley, 94720 CA*
[c]*Materials Science Division, Lawrence Berkeley National Laboratory, Berkeley, 94720 CA*
[d]*Chemical Science Division, Lawrence Berkeley National Laboratory, Berkeley, 94720 CA*
[e]*Department of Electrical Engineering and Computer Science, University of California, Berkeley, CA 94720*

Received 1 July 2005; accepted 24 August 2005

High-density arrays of platinum nanowires with dimensions 20 nm × 5 nm × 12 μm (width × height × length) have been produced on planar oxide thin films of silica, alumina, zirconia, and ceria. In this multi-step fabrication process, sub-20 nm single crystalline silicon nanowires were fabricated by size reduction lithography. The Si nanowire patterns were then replicated to produce a high density of Pt nanowires by nanoimprint lithography. The width and height of the Pt nanowires are uniform and are controlled with nanometer precision. The Pt surface area is larger than 2 cm^2 on a 5 × 5 cm^2 oxide substrate. The catalytic oxidation of CO was carried out on zirconia-supported Pt nanowires. The reaction conditions (100 Torr O_2, 40 Torr CO, 513–593 K) and vacuum annealing (1023 K) did not change the nanowire structures.

KEY WORDS: platinum nanowires; two-dimensional model catalysts; oxide-supported platinum nanowires.

1. Introduction

Transition metal catalysts usually consist of nanoparticles in the 1–100 nm size-range deposited on high surface-area supports. The particle size, surface structure and the oxide–metal interface all influence catalytic activity, selectivity, and resistance to deactivation. Model metal catalysts, usually in the form of single crystals, have been used with success to elucidate many of the atomic scale ingredients that influence, catalytic performance. Single crystals, however, lack the oxide–metal interface and small particle sizes of an industrial catalyst. So, there has been much effort to develop a model system that offers a choice of oxide–metal interface as well as control over metal structures on a nanometer scale. Several methods have been reported to prepare 2-D model nanoparticle catalysts, including laser ablation [1], spin coating of metal salt solutions on oxide supports followed by calcinations [2], evaporation of metal onto an oxide support [3–5], soft landing of size-selected clusters onto a planar support [6,7], decomposition of transition metal carbonyls [8], laser interference nanolithography [9], photolithography [10], colloidal lithography [11], and electron-beam lithography [12] (EBL). However, all of the above listed methods have deficiencies: (1) Non-lithography methods were able to access the catalytically interesting size regime but were not able to exert precise control over the size and surface structure of the model catalyst, (2) photolithography methods used previously were not able to access the catalytically interesting size regime (1–100 nm), (3) the serial nature of EBL makes it slow and costly. This report describes the fabrication of dense arrays of platinum nanowires deposited on oxide thin film surfaces of ZrO_2, SiO_2, Al_2O_3, and CeO_2. These samples have been fabricated by combining sub-lithographic nanofabrication [13] and nanoimprint technology [14,15]. The techniques used to produce these platinum model catalysts are described. The nanowire dimensions are uniform and are controllable with nanometer precision. The typical dimensions of a single nanowire are 20 nm × 5 nm × 12μm (width × height × length). So on a 5 × 5 cm^2 flat substrate, a total of 8×10^8 nanowires can be fabricated, which gives a total exposed metal surface area larger than 2 cm^2. The catalytic activity, and chemical and thermal stability of these model catalysts are demonstrated by carrying out catalytic oxidation of carbon monoxide at high reactant pressures and temperatures on the zirconia-supported Pt nanowires.

2. Fabrication of platinum nanowires on oxide surfaces

2.1. Fabrication of a single crystalline Si mold by size reduction lithography (SRL)

A detailed description of SRL can be found elsewhere [16,17]. The SRL process is shown schematically in figure 1a. Briefly, a 50-nm hard mask oxide (SiO_2) is thermally grown on a Si(100) wafer. A 120-nm

* To whom correspondence should be addressed.

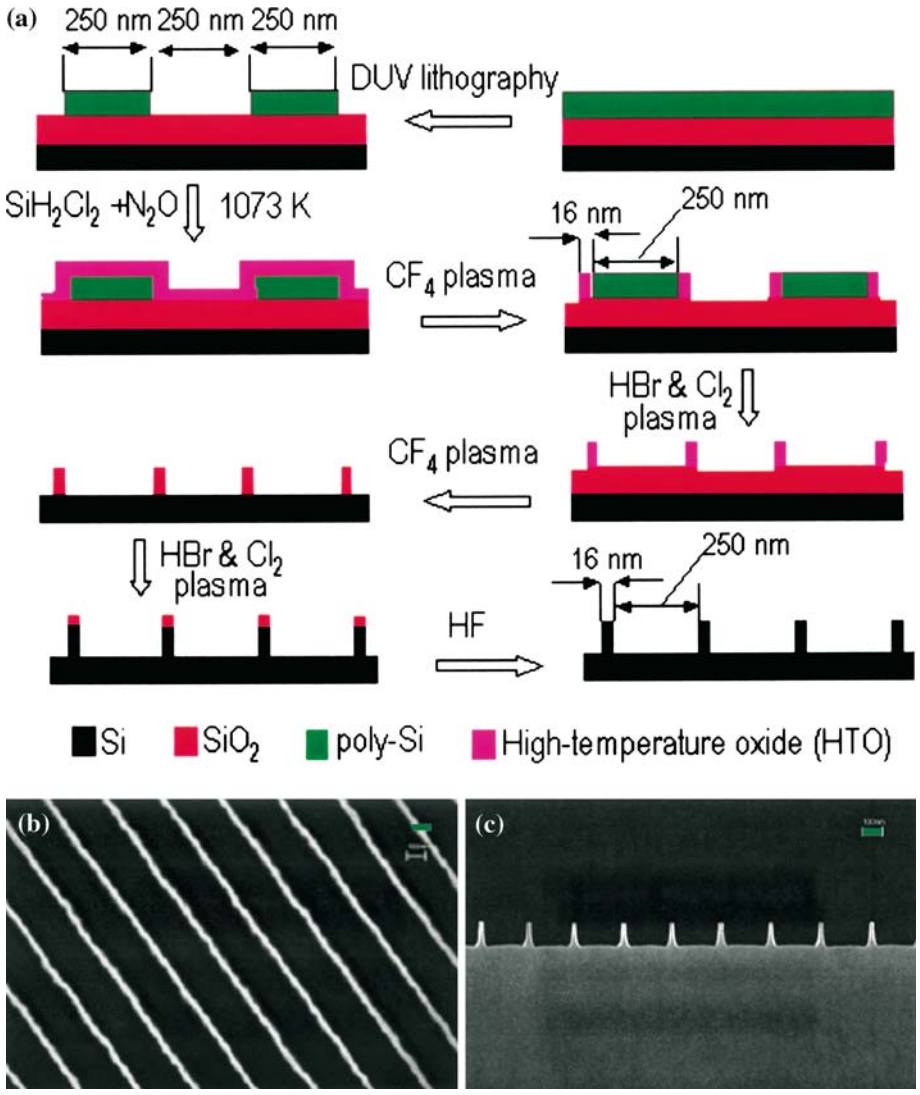

Figure 1. (a) Shematic drawing of the spacer lithography process (b) and (c) SEM top and cross-section views of the final nanostructures, which are used as an imprint mold. The Si wires mold has features of 16 nm and 110 nm high with 250-nm pitch. The green bars is 100nm.

polysilicon film is deposited on the hard mask oxide by low-pressure chemical vapor deposition (LPCVD) of silane. The polysilicon serves as a sacrificial layer to support and hold the sidewall spacers. The polysilicon layer is then patterned by deep-UV lithography (DUV) and plasma reactive ion etching (RIE) to form 0.25-μm wide, 12-μm long polysilicon line pattern with 0.25-μm spacing between lines.

A 10-nm thick high-temperature silicon oxide (INTO) film is then conformally deposited onto the patterned polysilicon by the LPCVD of SiH_2Cl_2 and N_2O. This coats both the tops and sidewalls of the patterned polysilicon layer. After the HTO is etched back anisotropically by CF_4 plasma, the polysilicon is exposed and is selectively removed by HBr and Cl_2 plasma etching. The selective removal of the polysilicon leaves 10-nm sidewall oxide spacers, which serve as an etching mask to pattern the underlying single-crystalline silicon. These relatively tall HTO spacers are transferred to the hard mask thermal oxide by CF_4 plasma. Next, the pattern is transferred into the Si(001) wafer by anisotropically etching in HBr and Cl_2 plasma. The residual thermal oxide mask is removed by buffered HF wet etching. Further size reduction of the silicon wires can be achieved by thermal oxidation, but this technique was not used here [17,18]. The principle of the SRL is based on the fact that material deposited during low-pressure chemical vapor deposition covers the step edge as well as the top of the step, known as conformal deposition. In contrast, plasma etching is an anisotropic technique, removing materials preferentially in the direction perpendicular to the surface. Therefore, by depositing a material that has a different etching rate than the sacrificial layer and directionally etching the material on the top of the step, the sacrificial layer can be removed selectively, leaving only the material deposited on the sacrificial structure sidewall. Thus the feature size generated is determined by the thickness of the deposited

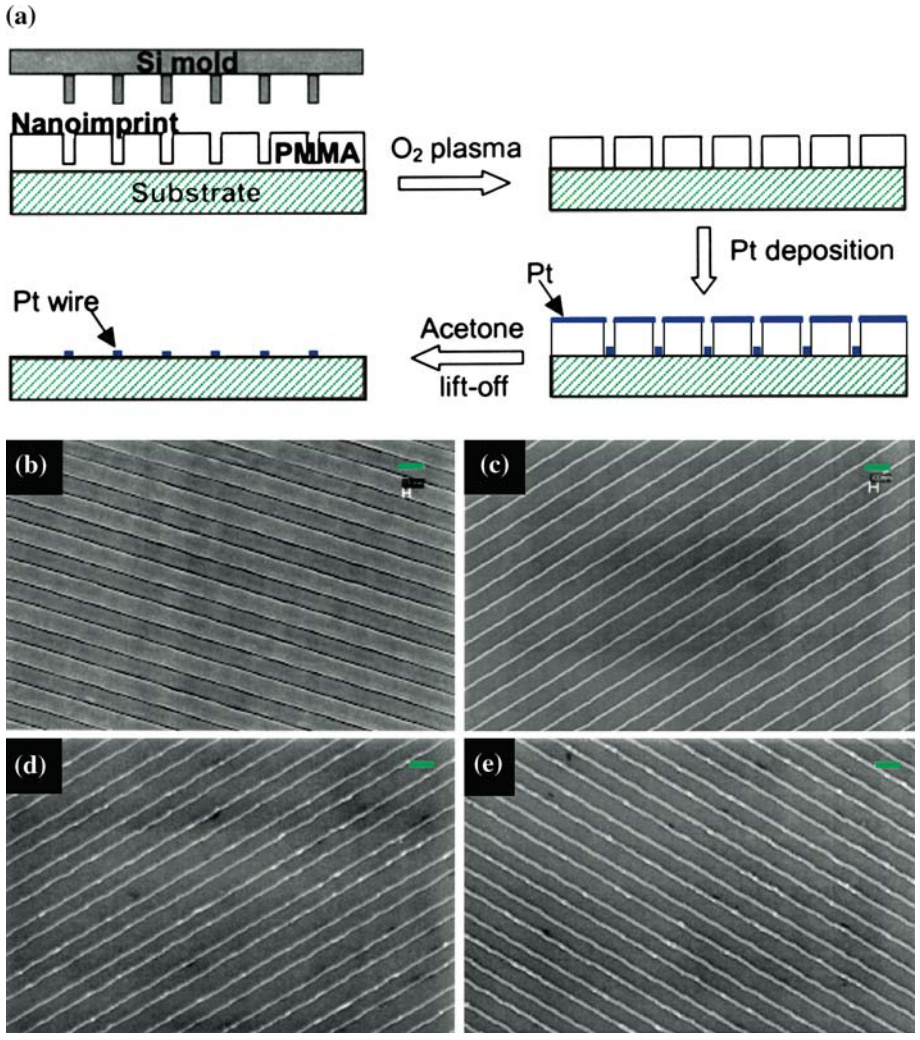

Figure 2. (a) Scheme of imprint process. (b) SEM top-view of the negative nanostuctures in PMMA resist as-imprinted. The trench width(18nm) is slightly larger than the wire width on the original(16nm). (c) to (e) SEM top-view of the Pt nanowires with of 20, 26 and 40 nm, respectively. The wire height can be easily controlled by depoisted Pt thickness. The green bars are 300 nm.

material not by the photolithography, but the pattern pitch is determined by the minimum feature size obtainable with photolithography. Because the thickness of the deposited film can be controlled to 10 nm or less with high precision, this method is capable of generating nanopatterns far smaller than possible by optical lithography. In this way we have batch-fabricated sub-20 nm Si wires from 250-nm patterns generated DUV photolithography (figure 1b and c).

2.2. *Fabrication of Pt wires by nanoimprint lithography (NIL)*

The single crystalline Si nanowire structures fabricated by SRL are used as a mold for producing high surface area Pt wires by nanoimprint lithography. The NIL process is shown schematically in figure 2a. Si(001) wafers covered by 100-nm oxide thin films are used as imprinting substrates, and the oxide thin films become the eventual supports for the Pt wires. The silica substrate is prepared by wet-oxidation ($H_2O_{(g)}$) of Si(001) at 1173 K. Alumina, zirconia and ceria oxide films are deposited onto native oxide covered Si(001) surfaces by electron-beam evaporation at a rate of 0.2 nm/s. The e-beam evaporator has a base-pressure 1×10^{-6} Torr and a beam collimation of $\sim$5 mrad. After deposition, the oxides are annealed at 1173 K for 4 h under oxygen ambient. Stoichiometric Al and Zr oxides are formed after oxygen annealing, but Ce sub-oxide (CeO_x) is revealed by XPS (not shown). Then PMMA thin films are spin-cast on the desired oxide surfaces. PMMA (M_w = 15 k) is dissolved in toluene at room temperature and kept in the solvent for 24 h to ensure complete dissolution of the PMMA. Before use, the solution is filtered by a 0.2 μm PTFE filter to remove undissolved polymer particles. Then, the solution is ultra-sonicated for 3 h to remove any dissolved gas. The film thickness is controlled by both the PMMA

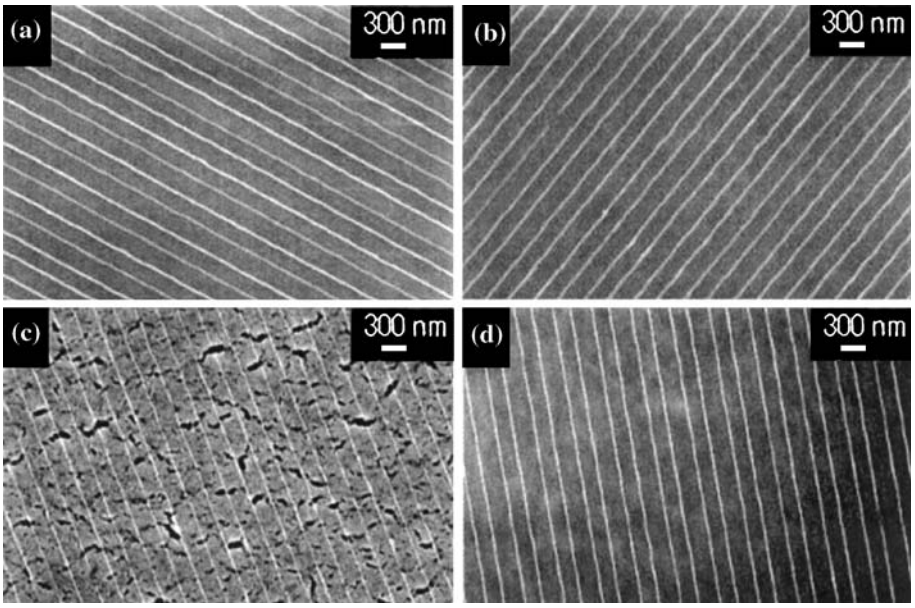

Figure 3. SEM images of 20-nm Pt nanowires on different oxide supports. (a) alumina; (b) ceria; and (d) Pt on zirconia after CO oxidation reaction.

concentration and spin rate. A typical 160-nm thick film is obtained by spin-casting an 8%, by mass, PMMA solution in toluene at 5600 rpm for approximately 30 s. Immediately after a film is spin-cast, it is baked at 423 K for 5 min to evaporate all residual solvent from the polymer layer. It is then cut to the size of the Si mold.

To facilitate the separation of the mold and PMMA-coated substrate after imprinting, the surface of the Si mold is functionalized by tridecafluoro-1,1,2,2-tetrahydrooctyl-1-trichlorosilane (FTS) to form a fluorine terminated self-assembled monolayer (SAM) before use. To form the SAM layer, the mold is first cleaned in piranha solution (98% H_2SO_4 + 30% H_2O_2) at 393 K to remove the organic contaminants, during which a thin layer of surface oxide and silanol groups form. Then the cleaned mold is transferred into an oven filled with 2 mTorr FTS at 363 K for 300 s. Water contact angle measurements show an angle larger than 105°, which verifies that the surface is functionalized. Functionalizing the surface lowers the surface energy and allows more facile separation of the mold from the PMMA-covered substrate.

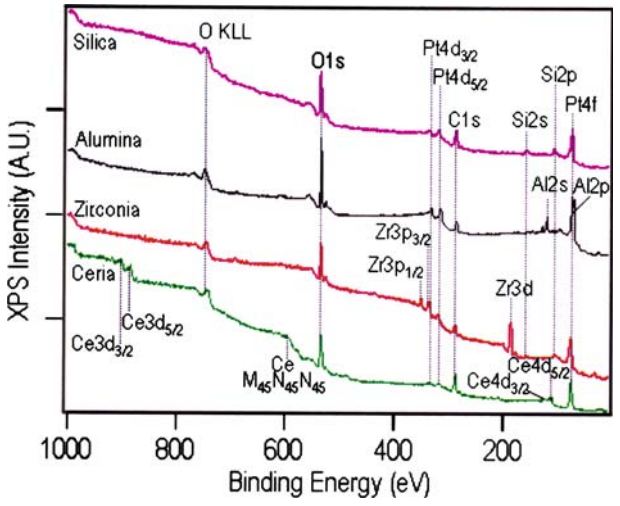

Figure 4. X-ray photoelectron spectra(XPS) of 20-nm Pt wires as-fabricated on various oxide supports. From top to bottom, the supports are silica, alumina, zirconia and ceria.

Finally the substrate and the mold, covered by PMMA and FTS, respectively, are brought into close contact. Upto this step, all processes are performed in a class-100 clean room environment to avoid possible dust contamination, which may ruin the conformal contact between the substrate and the mold. The samples are imprinted under 4000 PSI at 393 K for 300 s using a home-made hydraulic press [18]. The imprint cell ($Z = 64$ mm) is heated resistively from room temperature to the imprinting temperature at ramp rate 2 K/min. The cell is vacuum-pumped by a mechanical pump to evacuate the vapors that the sample outgases during heating and pressing. After the imprint, the sample is air-cooled to room temperature under pressure, and the substrate and mold are manually separated.

The top-view SEM image of an imprinted PMMA film is shown in figure 2b. The width of the trenches is about 2 nm larger than the dimension of the original Si wires. It is believed that the broadening is not the result of the imprinting process but the FTS SAM cover layer. Cross-sectional SEM (not shown) of the as-imprinted sample shows that there is still residual PMMA at the bottom of the imprinted trenches, which is eliminated by anisotropically etching the substrate in O_2 plasma. Due

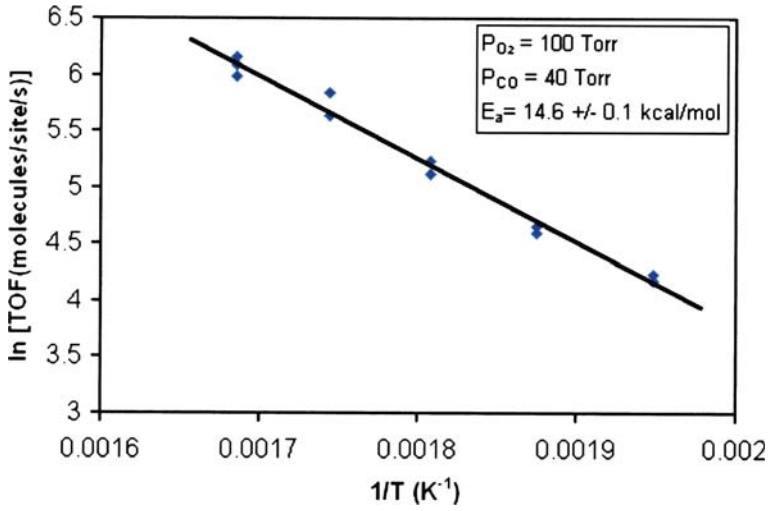

Figure 5. Arrehenius plot of CO oxidation carries out on zirconia-supported Pt nanowires.

to an isotropic contribution to the PMMA etching, i.e., the etching is not perfectly perpendicular to the substrate, the trench width in the PMMA is increased by a few nanometers. The broadening caused by the isotropic etching can also be utilized to produce different width Pt wires, and even bimodal size distribution wires [19]. After the residual PMMA is removed, platinum is deposited at a rate of 0.1 nm/s by e-beam evaporation. The Pt that is in contact with only PMMA is lifted-off by acetone assisted with ultrasonication as shown in figure 2a, and the Pt deposited through the imprinted pattern and onto the silica forms nanowires (figure 2b–e). The width of Pt wires is controlled by the initial silicon wire width in figure lb and c, and by the isotropic etching effect during O_2 plasma breakthrough of PMMA. The height of Pt is controlled by the thickness of deposited Pt, which is monitored *in situ* by a crystal oscillator and calibrated by atomic force microscopy (not shown). The upper limit is quarter of the depth of the imprinted PMMA trenches (~25 nm). A Pt film thicker than this will cause difficulties during the lift-off. The lower limit of the wire height is determined by the sensitivity of the crystal oscillator (0.1 nm), which gives a sub-monolayer Pt film. Using the same techniques, 20-nm wide 5-nm high Pt wires are fabricated on alumina, zirconia and ceria surfaces (figure 3a–c).

3. CO oxidation catalyzed by Pt nanowires on zirconia

A full study of CO oxidation catalyzed by the Pt nanowires on various oxides is beyond the scope of this letter, and will be published in another paper. Here, the oxidation of CO on ZrO_2-supported Pt nanowires is reported. The reaction studies are carried out in an ultrahigh vacuum (UHV) equipped with a high-pressure cell. The general design of this type of chamber has been described elsewhere [20,21]. The outer chamber achieved a working pressure of 1×10^{-9} Torr between reactions. The sample is mounted on a ceramic heater (Advanced ceramics, HT-01) with Ta clips. The sample temperature is measured with a K-type thermocouple clamped to the edge of the sample. The sample is initially cleaned by the cycles of 1×10^{-6} Torr NO_2 at 573 K for 30 min, to remove carbonaceous contaminants from the platinum surfaces, and annealed under vacuum at 1023 K for 30 min. Between reaction runs, the surface is cleaned by dosing 1×10^{-6} Torr NO_2 at 573 K for 20 min. The sample cleanliness is verified by AES.

During sample cleaning in NO_2, the reaction gases are mixed in a gas manifold. Upon completion of the cleaning, the mixed gases are introduced to the reaction loop. In the reaction loop, the gas mixture consists of 100 Torr O_2, 40 Torr CO, and 620 Torr He. The purities of O_2, CO, and He gases used in reaction studies are 99.997, 99.99, and 99.9999%, respectively. All gases are used as received from Airgas without further purification. The gases are circulated through the reaction line by use of a Metal Bellows recirculation pump at a rate of 2 L/min. The volume of the reaction loop is 0.225 L. A HP Series II gas chromatograph (GC) equipped with a TCD detector and a $15' \times 1/8''$ SS 60/80 Carboxen-1000 (Supelco) is used to separate and analyze products. The GC is part of the reaction loop and samples the circulating reaction gases every 5 min using an automatic sampling valve.

CO oxidation reactions are carried out in the temperature region of 513–593 K. The results are presented in an Arrhenius plot (figure 5). The apparent activation energy of the reaction is measured to be 14.6 ± 0.1 kcal/mol, and the turnover frequency is 1.5×10^3 molecules/site/s at 573 K, consistent with literature results [22]. After CO oxidation, SEM (figure 3d) is taken *ex situ* to monitor any possible morphology change of the nanowire catalyst. Comparing figure 3c

and d, the nanowires show no noticeable change in terms of dimensions and locations after 1023 K vacuum annealing and high pressure CO oxidation up to 593 K.

4. Summary

We have demonstrated the capability to fabricate Pt nanowires on large planar silica, alumina, zirconia and ceria surfaces (5×5 cm^2). However, these fabrication techniques are not limited to these materials and can be applied to many other systems. The wire height and width are precisely controlled in the range of 1–25 and 20–40 nm, respectively. The kinetics of CO oxidation catalyzed by zirconia-supported Pt nanowires are shown to be similar to those seen on Pt(111). Shown by SEM, the Pt nanowire feature dimensions and placement remain the same after sample cleaning and CO oxidation.

Acknowledgment

This work was supported by the Director, Office of Energy Research, Office of Basic Energy Sciences, Chemical Sciences Division, of the U.S. Department of Energy under Contract No. DE-AC02-05CH11231.

References

[1] Z. Paszti, G. Peto, Z.E. Horvath, A. Karacs and L. Guczi, Phys. Chem. B 101 (1997) 2109.
[2] R.M. van Hardeveld, P.L.J. Gunter, L.J. Van Uzendoorn, W. Wieldraaijer, E.W. Kuipers and J.W. Niemantsverdriet, Appl. Surf. Sci. 84 (1995) 339.
[3] X. Lai, T.P St. Clair, M. Valden and D.W. Goodman, Prog. Surf. Sci. 59 (1998) 25.
[4] J. Hoffmann, S. Schauermann, J. Hartmann, V.P. Zhdanov, B. Kasemo, J. Libuda and H.-J. Freund, Chem. Phys. Lett. 354 (2002) 403.
[5] J. Libuda and H.-J. Freund, J. Phys. Chem. B 106 (2002) 4901.
[6] U. Heiz, A. Sanchez, S. Abbet and W.D. Schneider, J. Am. Chem. Soc. 121 (1999) 3214.
[7] H.V. Roy, P. Fayet, F. Patthey, W.-D. Schneider, B. Delly and C. Massobrio, Phys. Rev. B 49 (1994) 5611.
[8] A.M. Argo, J. Odzak, F.S. Lai and B.C. Gates, Nature 415 (2002) 623.
[9] M. Schildenberger, Y. Bonetti, L. Aeschlimann, M. Scandella, J. Gobrecht and R. Prins, Catal. Lett. 56 (1998) 1.
[10] A.C. Krauth, K.H. Lee, G.H. Bernstein and E.E. Wolf, Catal. Lett. 27 (1994) 43.
[11] C. Werdinius, L. Osterlund and B Kasemo, Langmuir 19 (2003) 458.
[12] J. Gaines, J. Zhu, E.A. Anderson and G.A. Somorjai, J. Phys. Chem. B 106 (2002) 11463–11468.
[13] B.D. Gates, Q. Xu, J.C. Love, D.B. Wolfe and G.M. Whitesides, Annu. Rev. Mater. Res. 34 (2004) 339.
[14] S.Y. Chou, P.R. Krauss and P.J. Renstrom, Science 272 (1996) 85.
[15] L.J. Guo, J. Phys. D: Appl. Phys. 37 (2004) R123.
[16] Y.K. Choi, J.S. Lee, J. Zhu, G.A. Somorjai, L.P. Lee and J. Bokor, J. Vac. Sci. Tech. B 21 (2003) 2951.
[17] Y.K. Choi, J. Zhu, J. Grunes, J. Bokor and G.A. Somorjai, J. Phys. Chem. B 107 (2003) 3340.
[18] J. Zhu, Ph.D. Dissertation, Chapter 5, (University of California, Berkeley, 2003).
[19] X.-M. Yan, S. Kwon, A.M. Contreras, J. Bokor and G.A. Somorjai, Nano Lett. 5 (2005) 745.
[20] J.C. Schlatter and M. Boudart, J. Catal. 24 (1972) 482.
[21] B. Segal, R.J. Madon and M. Boudart, J. Catal. 52 (1978) 45.
[22] X. Su, P.S. Cremer, Y.R. Shen and G.A. Somorjai, J. Am. Chem. Soc. 119 (1997) 3994.